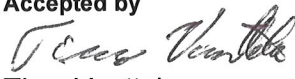# Chemical effects in the sump water pool during post-LOCA conditions – literature review

Authors: Tiina Lavonen

Confidentiality: Public

Report's title	
Chemical effects in the sump water pool during post-LOCA conditions – literature review	
Customer, contact person, address	**Order reference**
SAFIR2014 Research Project	12/2013SAF
Project name	**Project number/Short name**
Chemistry of fission products in containment (FISKES)	81524/FISKES2013
Author(s)	**Pages**
Tiina Lavonen	33
Keywords	**Report identification code**
Chemical effects, LOCA, PWR, precipitation, strainer blockage	VTT-R-01126-14

Summary

This report is part of FISKES (Chemistry of fission product in containment building) project within the SAFIR2014 research programme (the Finnish public research programme on nuclear power plant safety). The aim of the project is to improve the knowledge of the chemistry in the case of severe nuclear power plant (NPP) accidents, such as loss of coolant accident (LOCA), especially in the containment pool environment. The goal of this literature review is to investigate the chemical effects, which take place in the containment pool environment, so that chemical effect information can be utilised in the Chempool modelling. Based on the information of this literature review, laboratory experiments will be planned and conducted to investigate the formation of precipitations, colloids and gels in containment pool environment especially found in the Finnish LWRs.

Based on the information found from literature the most important features that effect on the precipitation during post-LOCA conditions are pH of the solution, insulation materials, pH buffer and corrosion of metal alloys, such as Al and Zn. Also temperature evolution during LOCA may have some effects on the chemical effects. Chemical effects that may occur during post-LOCA environment depend highly on plant specific conditions and therefore the evaluation of chemical effects must be done for each plant design and conditions separately.

Confidentiality	Public

Espoo 7.3.2014

Written by	Reviewed by	Accepted by
Tiina Lavonen, Research Scientist	Merja Tanhua-Tyrkkö, Research Scientist	Timo Vanttola, Head of Research Area

Distribution (customer and VTT)
SAFIR2014 RG5, Timo Vanttola, Kaisa Simola, Vesa Suolanen

Contents

1. Introduction

This report is part of FISKES (Chemistry of fission product in containment building) project within the SAFIR2014 research programme (the Finnish public research programme on nuclear power plant safety). The aim of the project is to improve the knowledge of the chemistry in the case of severe nuclear power plant (NPP) accidents, such as loss of coolant accident (LOCA), especially in the containment pool environment. The goal of this literature review is to investigate the chemical effects, which take place in the containment pool environment, so that chemical effect information can be utilised in the Chempool modelling. Based on the information of this literature review, laboratory experiments will be planned and conducted to investigate the formation of precipitations, colloids and gels in containment pool environment especially found in the Finnish LWRs.

Before the 1990's chemical effects, screen and strainer blockage and subsequent head loss were not considered as a design and operational issue in light water reactors (LWR). The post-LOCA containment and recirculation water were assumed to be generally clean. Also, the LOCA-generated fibrous debris was not considered to exhibit filtering behaviour. However, after 1992 strainer blockage incident in Sweden Barsebäck BWR the issue has become a real concern and it has been studied widely. Also many operators have chosen to replace the old sump screens and suction strainers with new larger ones. (Hart, 2004)

After LOCA incident, particulate and fibre mix is suspended in the post-LOCA suppression pool water, which flows to the emergency core cooling system (ECCS) suction strainers. Fibre debris forms thin layer on the strainer and filtrates the particulate material. The studies have shown that it is either very likely or likely that sump screens or trainers become blocked with the mixed debris, which could results into a loss of recirculation water flow. (Hart, 2004) The water flow restriction at the strainer may also threaten the safety margin that is required to ensure the successful operation of ECCS and containment spray system (CSS) pumps (Bahn, 2013). Dissolved particulate and electrolytes increase bulk fluid viscosity, which may result in increased head loss through the debris bed and small debris that flows through the sump screens can damage the coolant recirculation pump and block the nozzles and valves of recirculation system (Chen et al., 2007). If the cooling water flow is stopped by the strainer blockage, serious consequences, such as core damage may occur (Bahn, 2013).

BWR particulate debris consists mainly of iron oxide, otherwise the particulate debris of BWR and PWR are similar, including paint chips, concrete dust, granular insulation particulate and also so called latent dirt and dust, which is not necessarily found in the plant documentation. The fibre debris consists of fibrous material created from thermal insulation and fireproofing material by LOCA forces, and also latent fibre. Tests have also shown that post-LOCA sprays react chemically with coatings and metals dissolving them to the recirculation cooling water. Further, the dissolved species can form precipitates, which are filtered by a fibre mat on a sump screen and can increase the head loss across the filtering mat significantly. (Hart, 2004) Formed chemical precipitates may also interact with fibrous debris bed and increase the head loss across the strainers (Bahn, 2013).

2. Chemical effects in PWR

After LOCA, recirculation of water could lead to chemical reactions, because of the presence of boric acid or Li hydroxide, which are used to control the reactivity of the reactor, and additives such as sodium or potassium hydroxide or trisodium phosphate (TSP) in the sump. Chemical reactions may lead to significant additional amount of debris and this debris may interact with the existing debris. Typical accumulation of fine fibrous debris on the strainer is presented in *Figure 1*. (NEA, 2013)

Figure 1. Typical accumulation of fine debris bed on the strainer (NEA, 2013).

At typical temperatures and pH values (pH close to 9 and T of the sump water 40 - 100 °C, local T higher < 350 °C may be detected) of post-LOCA conditions, corrosion of metals (aluminium, zinc) occurs and reaction is temperature-dependent. These dissolved metals in the sump water have relatively low solubility limits and can form gelatinous precipitates, which can be transported with the water flow. (NEA, 2013) The combination of these chemical reactions is known as 'chemical effects'.

Chemical effects have two key processes:
1. Release of various chemical species into the sump water by corrosion or dissolution
2. Chemical reactions between these various dissolved species leading to the formation of precipitate.

The list of the materials that can undergo corrosion or dissolve is long and the most important features that have effect on these reactions are temperature and pH. The materials that can react are metals, concrete and different insulators. *Table 1* presents some of the materials found in containment (NEA, 2013).

Table 1. Debris materials and possible corrosion products, which are possible reactants in sump water (Choromokos et al., 2010; NEA, 2013).

Metals, carbon steel, galvanised steel, metal coatings	Al, Zn, Fe, Ni, S, Cu
Concrete	Ca, Si, Al
Insulators (fibreglass, calcium silicate, etc.)	Si, Al, Ca, Mg, B, alkalis
Primary cooling loop water	B, Li, Na, organics
pH buffers (TSP, HCl, NaOH, NaTB)	Na, PO_3, Cl, B

The solution condition in sump water after LOCA is also important feature that determine the reactions that take place. Especially, pH and concentration of chemistry control reagents are the key features. After LOCA, the pH evolution depends highly on what chemical buffering is used to minimise iodine release. The sump water contains 2500 ppm boric acid solution, (boron used as a neutron moderator) and soda, released from another tank, in order to create alkaline solution (minimise the airborne iodine release), with the target pH around 9.3. (Sandrine et al., 2008) In Finnish PWR and BWR, KOH is used and expected pH is between 8 and 9. (NEA, 2013)

As materials undergo corrosion or dissolution, at some point plateau is reached. This is because of the surface passivation or the solubility limit of dissolved species is reached. Surface reaction can either inhibit or accelerate the release of species. Under extreme conditions (pH > 9 and temperature 100 - 350 °C), dissolution or corrosion cannot be inhibited, and therefore release can be linear with time, which may lead to a mixture of dissolved metals and particulates. (NEA, 2013)

After the solubility limit of dissolved species is reached, precipitates will form continuously in the solution and onto all wetted surfaces until the source term is depleted. In the post-LOCA sump, there are large surface areas in containments and debris, where dissolved species can precipitate via heterogeneous nucleation. Heterogeneous nucleation is surface reaction, where molecules of the solution react with suitable surface and form precipitate on the surface. Heterogeneous nucleation usually occurs at lower degrees of supersaturation. (NEA, 2013)

To reach the solubility limits of dissolved species, various corrosion and dissolution reactions are required. Therefore, precipitation reactions require some time after the beginning of accident before they occur. The solubility limit can be exceeded in two ways. Whether at constant pH and T, concentration of dissolved species is increased until the dissolution limit is exceeded, or a change in conditions (e.g. T or concentration) leads to a decrease of the solubility of precipitating phase. In the second case, much higher degree of supersaturation can occur. (NEA, 2013)

Post-LOCA conditions are far from equilibrium conditions. Physical and chemical conditions of the system change with time, therefore prediction of conditions and precipitate formation is complicated and thermodynamic models do not give accurate predictions. More likely, precipitation is dominated by supersaturation, heterogeneous nucleation, colloid stabilisation and gel formation. Therefore precipitated phases are often amorphous or poorly crystallised, and are significantly more soluble than well crystallised thermodynamically more stable solids. Also the time scale of the transformation of the amorphous phases to more stable phases may be significantly longer than the period of coolant recirculation. (NEA, 2013)

Precipitation can also be delayed by kinetic strains, even if the solubility limit is reached. Most often metastable phase or phases with higher solubility are formed, before the actual more stable phase is formed. Therefore, concentration in solution may be higher than it could be predicted if only the precipitation of the most stable phase is included. Some compounds may have slow formation kinetics and therefore they do not occur even if thermodynamical models would predict so. (NEA, 2013)

3. Release of chemical precipitants and precipitation

3.1 Aluminium

Al has low corrosion rate at pH 4 – 7, but at lower and higher pH corrosion rate is significantly higher due to the increasing solubility of the aluminium surface oxides. Higher temperature has been reported to increase the solubility. Soluble Al species at high and low pH values are Al^{3+}, $Al(OH)^{+2}$, $Al(OH)_2^+$ and $Al(OH)^-$. At pH range between 4 and 9, a small pH change towards neutral point leads to rapid and voluminous formation of colloidal Al hydroxide, which forms readily gel containing water and anions. These anions may stabilise or destabilise colloids. *Figure 2* presents the monomeric Al hydrolysis species (NEA, 2013).
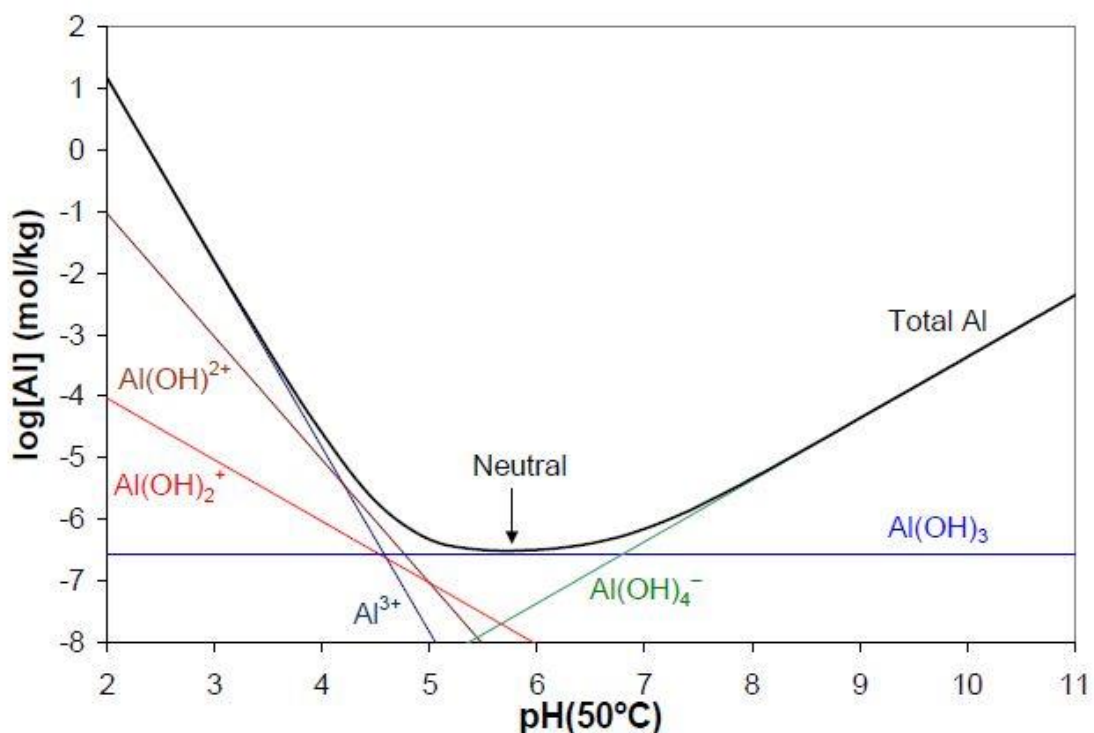
Figure 2. Al hydrolysis species in equilibrium with gibbsite (Al(OH)₃) as a function of pH at 50 °C (NEA, 2013).

It has been noticed in laboratory experiments, that there is two competing processes at the surface of Al metal; direct dissolution and electrochemical formation/dissolution of Al hydroxide films. First process is intense and results in high corrosion rate, but after the film has been formed it serves as a barrier, which reduces the species transport significantly and therefore also the corrosion rate. Generally, Al oxide layer has better oxidation resistance and slower oxidation rate than other metal oxide layers, especially in neutral environment. (Zhang et al., 2009)

3.1.1 Aluminium dissolution in alkaline environment of sump water

Metal parts in nuclear power plant containments and fiberglass and other insulators contain often aluminium. pH at post-LOCA emergency core cooling system is close to 9 or 10, so therefore the chemistry and corrosion behaviour of Al in alkaline solutions is important. *Zhang et al.* have reviewed extensively the special features in aluminium-alkaline system.

At pH > 9, $Al(OH)_4^-$ is dominant species. Therefore in alkaline environment, dissolution of Al species is a function of aluminium hydroxide phase and direct dissolution follows the reaction presented in *Eq 1* (Zhang et al., 2009):

$$Al + 3\ H_2O + OH^- \rightarrow 3/2\ H_2 + Al(OH)_4^- \tag{1}$$
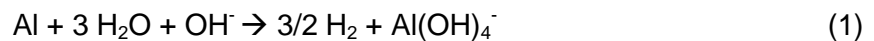
However, Al corrosion after the Al oxide film has been formed follows the reaction presented in *Eq 2* (Zhang et al., 2009):

$$Al_2O_3 + 2\ OH^- + 3\ H_2O \rightarrow 2\ Al(OH)_4^- \tag{2}$$
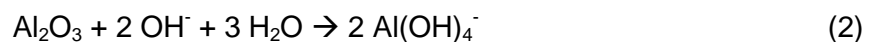
In alkaline solution, oxide layer may transform to hydroxide layer due to the attachment of OH^- ions (Eq 3) and then the Al corrosion follows *Eq 4* (Zhang et al., 2009):

$$Al(ox) + 3\ OH^- \rightarrow Al(OH)_3 \tag{3}$$

$$Al(OH)_3 + OH^- \rightarrow Al(OH)_4^- \tag{4}$$

Corrosion rate of Al is dependent on the flow velocity as presented in *Figure 3* (Zhang et al., 2009).
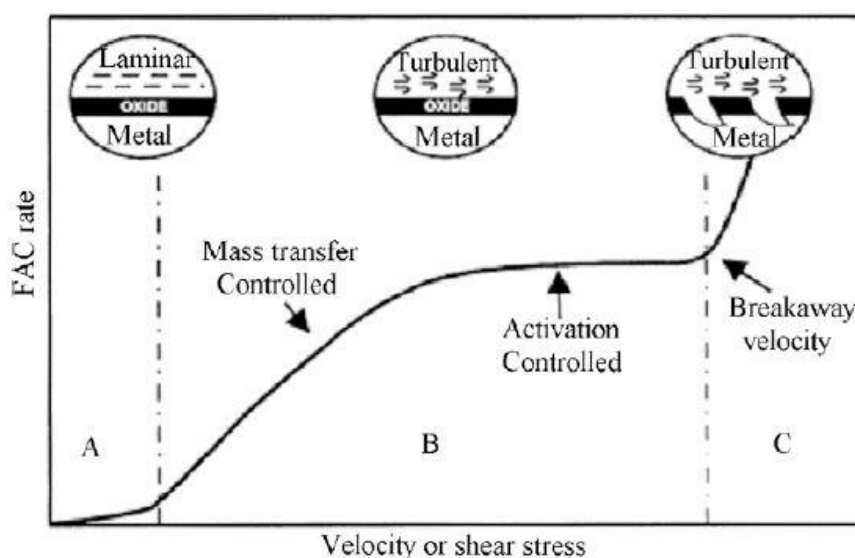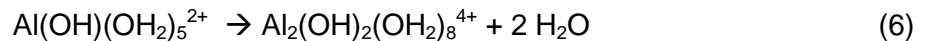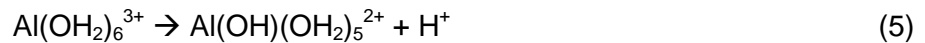

Figure 3. Metal corrosion rate dependence on the flow velocity of the solution (FAC =Flow Accelerated Corrosion) (Zhang et al., 2009).

Al dissolution in alkaline environment may be inhibited by organic or inorganic species present in the solution. Organics, such as benzoin acids, citric acid and other organic acids inhibit the Al dissolution due to the acid adsorption. For the inorganic inhibitors, $H_2PO_3^-$ has been reported to have inhibition efficiency about 97 %. However, other inorganics act as activators, for example NaCl, $NaNO_3$, Na_2SO_4, $NaIO_3$ are activators. Also silicates have been found to be effective inhibitors for Al corrosion and this is very useful in reactor environment, where silicate containing insulation materials are present. Inhibition is reported to due to the amorphous aluminosilicate film formation on the metal surface. (Chen et al., 2007; Zhang et al., 2009; NEA, 2013) However, according to the *in situ* experiments of *Chen et al.* silicate inhibition is efficient only when cal-sil is used as the main insulation material, fibreglass alone is not sufficient source of silicate (Chen et al., 2007).

3.1.2   Precipitation of aluminium

It has been suggested in various studies that often in supersaturated solutions amorphous Al hydroxide is formed first, which undergoes different ageing processes towards more stable and ordered phase with lower solubility (Zhang et al., 2009). Crystalline Al hydroxide phases may be such as gibbsite ($Al(OH)_3$), bayerite ($Al(OH)_3$), nordstrandite ($Al(OH)_3$), boehmite ($AlO(OH)$) or pseudoboehmite (colloidal boehmite) and their formation depends on the temperature, pH and time. Solubility of precipitates decreases with increasing temperature and aging effect. Also increasing temperature results in pH decrease, which is due to precipitation and formation of double hydroxide bridges (Eq 5 and Eq 6) (NEA,2013).

$$Al(OH_2)_6^{3+} \rightarrow Al(OH)(OH_2)_5^{2+} + H^+ \tag{5}$$

$$Al(OH)(OH_2)_5^{2+} \rightarrow Al_2(OH)_2(OH_2)_8^{4+} + 2\ H_2O \tag{6}$$

This reaction has also generally accepted to be rate-limiting step in Al hydroxide formation in slight alkaline conditions. Therefore, aluminium hydroxide aging or transition to more stable phase has strong dependence on OH/Al ratio and temperature. However, pH and Al concentration in the solution also affects the aging effect, so that aging may take place via metastable form before the crystalline phase is formed. (NEA, 2013) Supersaturation level of solution affects the crystallinity and the transformation of the precipitate. At high supersaturation levels amorphous less stable phases are formed first, which undergo transformation to more crystalline and stable forms. At lower supersaturation levels, more crystalline and stable form of the precipitate is formed right away without the transformation steps. (Zhang et al., 2009)

In addition to Al hydroxides and oxyhydroxides, aluminium may be included in precipitates such as Al phosphate, Ca-Al phosphates or aluminium silicates. The formation of precipitation and its properties are dependent on T, pH, solution chemistry and the presence of solid surfaces (e.g. debris bed). Often in laboratory experiments, the concentration of dissolved Al is higher than the solubility of gibbsite at similar temperature. Due to these high concentrations, some of Al precipitates as non-crystalline material with carbonate, boron and sodium. The presence of some organic ligands or anions, such as citric acid, fulvic acids, sulfate or silic acid, has been reported to slow down or even prevent totally the formation of Al hydroxide phase. (Zhang et al., 2009)

Boric acid is used as pH buffer to reduce iodine release and also as reactivity control in PWR primary water loop, so therefore the aluminium-boron interactions are important in the post-LOCA conditions. At pH < 7, boron exists mainly as undissociated boric acid, and at high pH above 10, metaborate $B(OH)_4^-$ is the prevailing boron species. However, between pH 6 and 11 and high concentrations, highly water soluble polyborate anions such as $B_3O_3(OH)_4^-$, $B_4O_6(OH)_4^-$ and $B_5O_6(OH)_4^-$ may be formed. At pH 9, approximately half of the total boron is in $B(OH)_3$ form and rest half in $B(OH)_4^-$ anion form. (Zhang et al., 2009)

Boron complex formation has been reported to increase Al solubility up to factors of 6 for gibbsite ($Al(OH)_3$) and boehmite ($AlO(OH)$). On to the aluminium hydroxide surface boron is present as specifically absorbed ion in the inner-sphere surface, which produces a shift in the mineral's zero point of charge to more acidic value. Which means that boron has effect on the surface behaviour of aluminium hydroxide, thus experiments done for aluminium hydroxide are not valid with surfaces where also boron is available. The absorption of boron on to the surface of Al hydroxide, inhibits the polymerisation process. Therefore, if boric acid is present Al corrosion rate is significantly higher than in the systems where boric acid is absent. (Zhang et al., 2009) *Bahn et al.* reported bounding estimates of Al solubility in basic solution containing boron (Figure 4). It has been also noted by *Chung et al.* that TSP (dissolving phosphate) can form a protective coating on the surface of Al and decrease Al release to some extent, but this was not effective for large amounts of Al and long spray duration. (Chung et al., 2011; NEA, 2013)
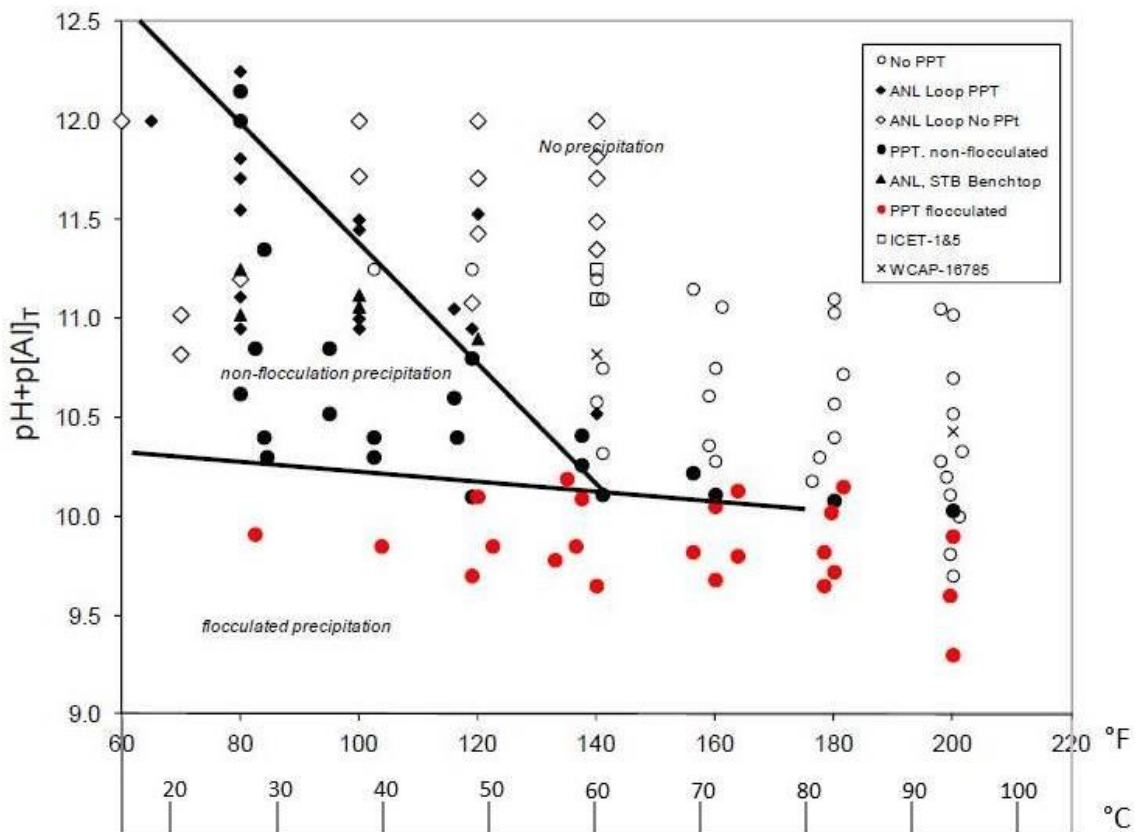

Figure 4. Conservative estimation of solubility of amorphous Al hydroxide in alkaline pH environment with boron. Open symbols indicate soluble species and solid symbols indicate precipitation. (PPT = precipitate, ANL = Argonne National Laboratory, STB = Sodium tetraborate, ICET = Integrated Chemical Effect Test, WCAP = Westinghouse Commercial Atomic Power) (Modified from Bahn, 2011a)

Chen et al. presented measured corrosion rates of aluminium in borated water from different authors. *Table 2* presents these results (Chen et al., 2008).

Table 2. Al corrosion rates in borated water (Chen et al., 2008)

Temp [°C]	Measured corrosion rate [g · m^{-2} · h^{-1}]	Borate concentration [mol · L^{-1}]	pH	Reference
50	0.15	0.1	9.2 – 9.3	Piippo et al., 1997
55	0.59	0.28	9.3 – 9.4	Griess et al., 1969
60	0.459	0.236	10	Jain et al., 2005
	0.986	0.259	10	
	1.01	0.236	10	
	1.22	0.236	10	
70	0.6	0.1	9.2 – 9.3	Piippo et al., 1997
90	1.45	0.1	9.2 – 9.3	Piippo et al., 1997
	1.89	0.259	10	Jain et al., 2005
	3.5	0.236	10	
100	8.9	0.28	9.3 – 9.4	Griess et al., 1969
110	1.23	0.1	9.2 – 9.3	Piippo et al., 1997
	2.2	0.259	10	Jain et al., 2005
	7.04	0.236	10	
130	3.06	0.1	9.2 – 9.3	Piippo et al., 1997

Table 2 results show the measured corrosion rates of aluminium in borated water with respect to temperature, borate concentration and pH. According to the results, higher temperature results in higher corrosion rate of Al. Borate concentration has significant effect on the measured corrosion rate of Al. Higher borate concentration increases the Al solubility in almost all cases. Some opposite results can be seen in the results with borate concentration of 0.259 mol/L and 0.236 mol/L, but this may result from the different analytical methods used for analysing the corrosion rate of Al (electrical resistance, polarisation resistance, current impedance or weight loss) and also the duration of the experiment. (Chen et al., 2008)

3.2   Silicon and calcium

The dissolution of glass contains hydronium diffusion into the glass and outward diffusion of alkali ions from the glass to the solution. Simultaneously, covalent silica network hydrolyses and dissolves. Silica bond Si-O-Si hydrolysis is slow at pH between 6 and 9. With longer exposure times, it has been noted that silicon dissolution is not linear and concentration in solution reaches plateau after certain amount of time. (NEA, 2013)

Compound structure, Ca/Si ration, pH, T and electrolyte concentration affect the Ca solubility. The amount of dissolved calcium depends on the dissolution of calcite, which is highly dependent on pH and phosphate concentration in the solution. (NEA, 2013)

3.2.1 Silicon and calcium solubility in alkaline environment of sump water

Two main sources of silicon in reactor pool are fibrous insulators and calcium silicate (cal-sil) and cal-sil is the main source. Silicon has been detected to be the dominant element in the sediment of sump pool, when fiberglass insulation material is used (Chen et al., 2007).

At pH 6.8 – 9.3 the dominant dissolved species is H_4SiO_4 at 25 °C. In pH range 9.5 – 9.9, both H_4SiO_4 and $H_3SiO_4^-$ are present. Increasing pH and temperature, increases the release of silicon. Fiberglass and solution composition have significant effect on Si dissolution. Buffer has significant effect on Si release, since complex formation may enhance or inhibit the dissolution. For example, formation of soluble oxides such as Al_2O_3 decreases Si release. It has also been suggested that boron may have impact on Si release; however it has not been studied much. (NEA, 2013)

Main calcium sources in sump pool are concrete, fibrous insulation and cal-sil and the latest is the most significant. When cal-sil is used as insulation material, calcium dominates over silicon in the sediment found in the sump pool. (Chen et al., 2007) The higher the Ca concentration in solution is, the lower is the Si concentration in solution. If cal-sil is not present, highest Ca release has been observed at pH 8.5 and lowest at pH 7. (NEA,2013)

Ca may also react with the buffer, which may inhibit or enhance the dissolution. The Ca release from concrete is the highest at low pH. Formation of protective calcium phosphate surface film on the surface of the concrete can also inhibit the Ca dissolution when TSP is present. (NEA, 2013) However, also cal-sil insulation material is needed so that sufficient calcium concentration in the solution is reached (Chen et al., 2007).

3.2.2 Precipitation and sedimentation

Water soluble silicon can form various monomeric and polymeric species depending on the pH of the solution (NEA, 2013). If soluble Al is also present, aluminosilicates can be formed via polymerisation. The type and Al/Si ratio of aluminosilicate depends on pH and initial Al/Si ratio in the solution. Also Al-Si compounds formed first are amorphous and transform to more stable crystalline phases with time. High pH increases the solubility of aluminosilicates. Also in acidic conditions, acid concentration destroys the framework of Al-Si compounds and therefore their solubility is highest at acidic conditions. Most often solubility minimum of Al-Si compounds is found near neutral pH area at low temperatures. Temperature affects also the solubility of aluminosilicates, however the effect is not yet well understood. *Mensah et al.* have studied the solubility of amorphous aluminosilicates and crystalline zeolite as a function of aluminium concentration and found that increasing Al concentration decreases the aluminosilicate solubility. However, even if the precipitation of aluminosilicates is thermodynamically favoured, it is kinetically unfavourable. Therefore it is often assumed that Al forms only hydroxide and oxyhydroxide precipitates. (NEA, 2013)

Calcium and phosphate ions can form many different kinds of sparingly soluble salts depending on the temperature, solute composition, pH and Ca/P ratio in the solution. Hydroxyapatite ($Ca_5(PO_4)_3OH$) has been found to be the least soluble and thermodynamically most stable phase in water at pH < 4. Therefore, hydroxyapatite is the first phase that is expected to precipitate from saturated solution. Also other metastable phases of Ca-P solids can be formed and all these precipitates tend to transform to more

stable phases such as hydroxyapatite. However, the kinetics of the transformation may be slow. pH has significant effect on Ca-P compound behaviour. From acidic conditions, the increasing pH results in decrease of solute Ca and P species in solution. Minimum of Ca phosphate solubility has been found to be at pH 8 – 10 at 25 °C. However, calcium phosphates have different dissolution behaviours in different temperatures. At temperature below 40 °C, calcium phosphate solubility decreases as the temperature increases. At pH 7, between 0 and 350 °C, extrapolated results suggest that the minimum of calcium phosphate solubility is near 50 °C (Figure 5) (NEA, 2013).
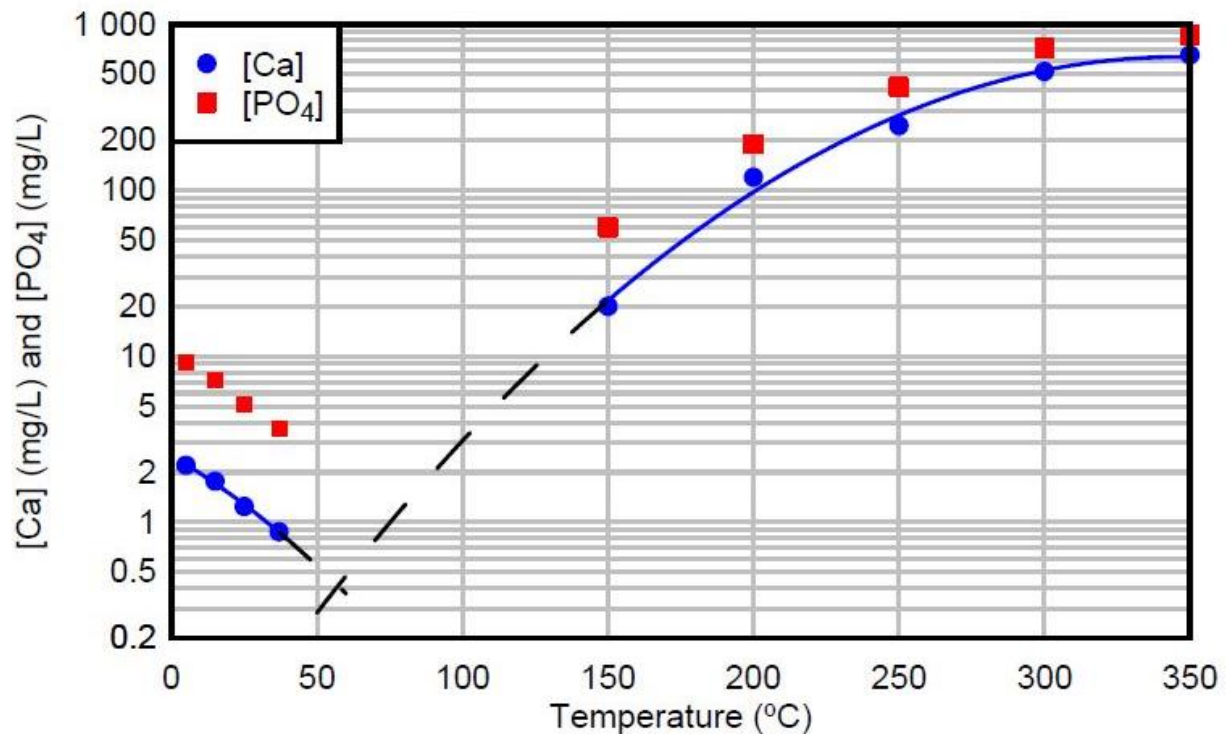

Figure 5. The concentration of dissolved Ca^{2+} and PO_4^{3-} species as a function of temperature. The solution is equilibrated with hydroxyapatite and pH is 7. (NEA, 2013)

In laboratory tests, including TSP and sump water containing cal-sil and fibreglass at pH 7 the formation of gel-like precipitate has been observed. It has been suggested that precipitate is most probably amorphous hydroxyapatite and $Ca_3(PO_4)_2$ (Chen et al., 2007). In tests with TSP, cal-sil and powdered concrete, calcium phosphate precipitated as a single phase or as a mixture with aluminium compound (Lane et al., 2008). However, tests have also shown that if excess cal-sil is not added to the solution, calcium release from fiberglass is not sufficient to form a precipitate. Tests with only TSP and powdered concrete have resulted to calcium phosphate precipitation only when the amount of concrete has been several orders of magnitude higher than in desired surface area to coolant volume ratio. Therefore concrete alone is also insignificant source of calcium. (Chen et al., 2007) On the contrary, *Chung et al.* reported that when TSP was added to the test solution, the head loss across the debris bed increased instantaneously, even if the calcium silicate amount was small (Chung et al., 2011; NEA, 2013).

3.3　Zinc

$Zn(OH)_2$ determines the solubility of Zn in water. The solubility of Zn is higher at neutral and high pH values. In alkaline conditions, solubility of Zn increases with increasing temperature. Minimum of the solubility is reached at about pH 10. Around pH 8.5 the temperature effect changes and at pH < 8 the higher temperature decreases the Zn solubility. (Figure 6) Therefore, in the post-LOCA sump water the formation of Zn corrosion products increases as temperature and pH decrease with time. (NEA, 2013)
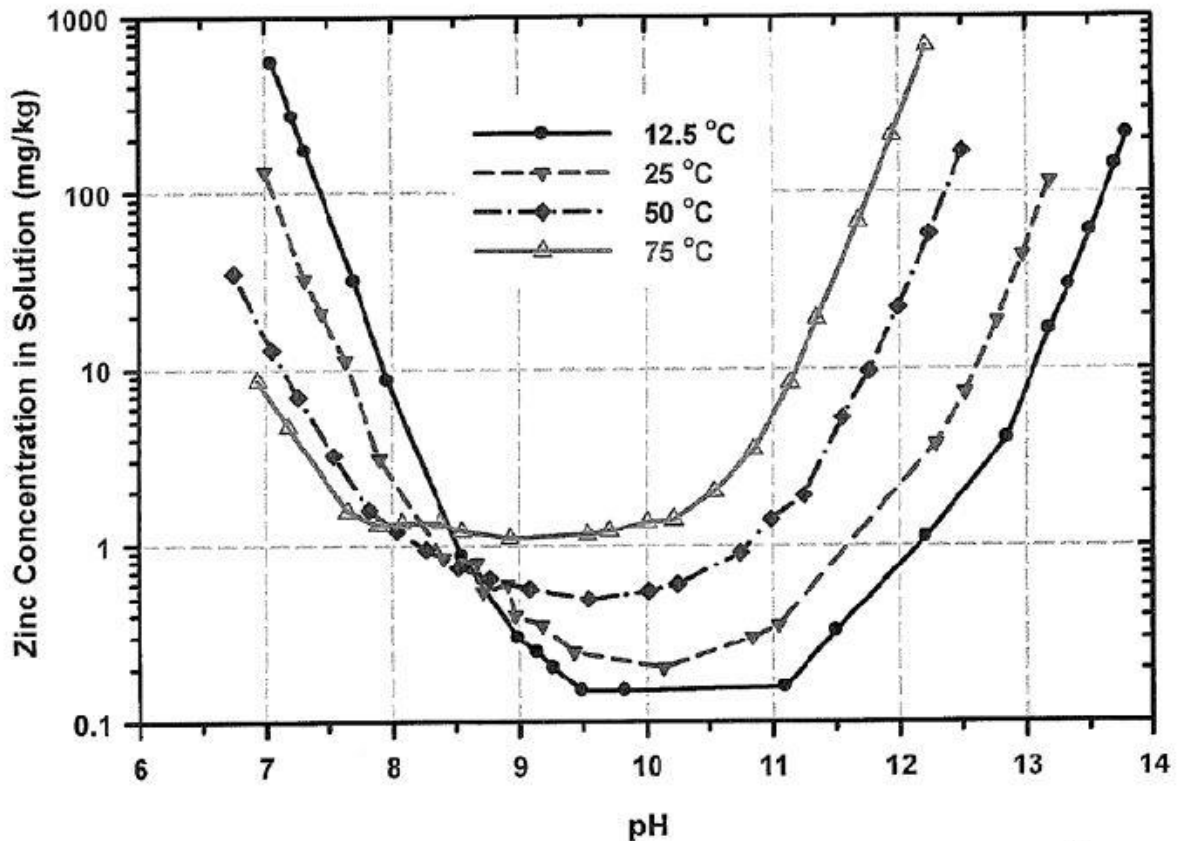
Figure 6. Solubility of crystalline $Zn(OH)_2$ as a function of pH and temperature (NEA,2013).

3.3.1　Zinc corrosion and precipitation in alkaline environment of sump water

Main sources of Zn are galvanised steel and Zn surface coating on other metals. Zinc corrosion can occur via two different reactions (Eq 7 and 8):

$$Zn + 2\ H_2O \rightarrow Zn(OH)_2 + H_2 \tag{7}$$

$$2\ Zn + O_2 + 2H_2O \rightarrow 2\ Zn(OH)_2 \tag{8}$$
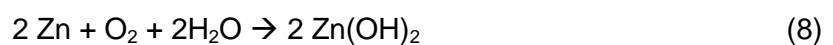
The corrosion film that forms on the surface of metallic zinc is most probably amorphous $Zn(OH)_2$, which has higher solubility than crystalline $Zn(OH)_2$. Generally, tests have shown that the corrosion and mobilisation of zinc are low compared to those of Al. Flow-induced corrosion without formation of solid corrosion products of Zn has been reported in Zn parts which have been directly exposed to a borated water shower. Zn coating may undergo

corrosion, due to the hydrodynamic impact of jet on the surface. Therefore, bare steel under the coating may begin to dissolve. Corrosion of steel may result in to the clogging of mineral wool fibre beds. The dissolution of Zn to coolant water causes small pH increase, which reduced further Zn and Fe dissolution. Similar, effect has been noticed when pH is increased by adding LiOH. Most important features that affect the Zn corrosion are coolant pH, T and the hydrodynamic jet impact of the coolant. Ratio of coolant volume to corrosion material surface area has significant effect on the strainer clogging. High Zn concentration in coolant water may lead to disadvantageous deposition of sparingly soluble zinc borate and its derivatives. (NEA, 2013)

4. Synergistic chemical effects

After LOCA, sump water pool environment is far from simple chemical environment. On the contrary, sump water contains a lot of different kinds of materials and corrosion products, which may react with each other. Some reactions may also be inhibited by soluble species and therefore it is hard to analyse which chemical reaction really take place.

To fully investigate the chemical effects in sump water pool, often *in situ* testing, modelling and single effects test are combined. Slow *in situ* testing including construction materials, debris and simulated sump water should be used for chemical effects testing. In this kind of tests, materials are allowed to corrode and dissolve to the sump water. Saturation concentration of dissolved species is reached slowly and species react and precipitate slowly over time. In this manner also inhibition and passivation can be included in the test. (NEA, 2013) Modelling can be used for example to characterise the precipitates that are formed. And later, single effects tests are used to recreate precipitates and single chemical effects detected in *in situ* testing.

To represent the synergistic chemical effects and all parameters that effect on them, example of *in situ* testing with results is presented in the following chapter.

4.1 *In situ* testing to evaluate the synergistic chemical effects

Dallman et al. and *Chen et al.* described the Integrated Chemical Effect Test (ICET) setting conducted in Los Alamos National Laboratory (LANL) in order to study the compatibility of different chemicals used in the ECCS following LOCA conditions and to analyse the chemical reactions and subsequent reaction products that may be generated in the containment sump during the post-LOCA conditions.

The test system included stainless steel test tank with heating element and spray nozzles, recirculation pump, flow meters, isolation valves and connection pipes. The chemical environment of post-LOCA was simulated with few variable parameters. In some tests fiberglass was only used as insulation material and in other tests fiberglass and calcium silicate insulation materials were both used. Also the pH buffer was varied between NaOH, TSP and STB and the pH was different in each test due to the different pH buffer. One of the test simulated an ice condenser reactor, which had different buffer and pH conditions. Representative amounts of Al alloy, copper, galvanised steel, carbon steel, inorganic zinc, concrete and insulation materials submerged or unsubmerged were included in the test settings. Also representative mounts of insulations materials, concrete particulate, cal-sil dust and latent debris were added to the simulant solution.

Test temperature was 60 °C, spray flow rate was 13 L per minute and the tests were run for 30 days with constant T and flow rate. Beginning of the tests included also 4 h spray phase to simulate the containment spray interaction with unsubmerged materials. Inductively coupled plasma atomic emission spectroscopy (ICP-AES), pH, turbidity, viscosity etc. analyses were made for the solution samples. Scanning Electron Microscope (SEM) and Energy-dispersive X-ray spectroscopy (EDS) were used for analysing the insulation and sediment samples, and also for the metal coupons during and after the test. Additionally, X-Ray diffraction (XRD) and X-Ray fluorescence (XRF) were used to analyse

the precipitates and sediment samples. (Chen et al., 2007) The condition and results of ICET are showed in the *Table 3*.

Table 3. ICET conditions and results (data from Chen et al., 2007).

Added to the simulant solution	Test 1	Test 2	Test 3	Test 4	Test 5
B [mg/L]	2800	2800	2800	2800	2800
NaOH [mg/L]	7677	-	-	9600	-
TSP [mg/L]	-	4000	4000	-	-
Buffer system	Borate	Phosphate	Phosphate	Borate	Borate
HCl [mM]	2.74	2.74	2.74	2.74	1.17
LiOH [mg/L]	0.7	0.7	0.7	0.7	0.3
Insulation [%] Fiberglass (NUKON) Cal-sil	100 -	100 -	20 80	20 80	100 -
Results					
Viscosity [mm^2/s]	0.515	0.498	0.500	0.520	0.476
pH	9.3 – 9.5	7.1 – 7.4	7.3 – 8.1	9.5 – 9.9	8.2 – 8.5
soluble Al [mg/L]	high, max 360	not detected	not detected	not detected	max 50
soluble Si [mg/L]	low	mainly low, at the end 75	nearly constant 100	increasing to the max 125	low
soluble Ca [mg/L]	low, max 15	low, max 10	increasing to the max 110	nearly constant 50	low, max 30
Amount of sediment [wet-g]	292	256	78,000	86,000	89
Precipitation	During the cool down, Al and B 86 % Na 8 % Ca 5 %	During the TSP addition, Ca 53 % PO$_4^{3-}$ 25 %			During the cool down, Al and B 79 % Na 8 % Ca 13 %

Viscosity of the simulant solution was relatively constant during the whole test and a bit higher than the viscosity of pure water (0.474 mm^2 /s at 60 °C). The higher electrolyte concentration increased the viscosity of the simulant water. Al concentration in the solution was highly dependent on the pH of the simulant solution. At lower pH values close to pH 7 Al was not detected, and at pH close to 8 and 9 Al was detected, especially at higher pH. Exception was detected in test 4 with pH 9.5 – 9.9 where Al was not detected. However, this result was explained by the fact that in this test the insulation material was mostly cal-sil and the passivation reaction of silicate in the solution.

Soluble silicate and calcium concentration correlated well with the presence of the cal-sil insulation material, however also the fiberglass released Si in the simulant solution at pH close to 7. In addition to cal-sil, calcium may be also released from concrete and fiberglass. pH has significant effect on Ca solubility, therefore there is higher Ca concentration in test 3 (pH ≈ 7) than that in test 4 (pH ≈ 9.5). TSP has been reported to inhibit the Ca dissolution from concrete, which may be the reason for low Ca concentration in test 2. However, the presence of TSP does not seem to have any inhibition effect in test 3, where cal-sil insulation material is present. However, later *Bahn* reported that detailed plant survey had suggested that the amount of cal-sil insulation used in ICET tests 3 and 4 may have been too high to be representative (Bahn, 2013).

X-ray and SED/EDS analysis of insulation material and sediment samples showed that particulate deposit amount correlated with the amount of generated sediment and that particulate material retained and attached on the fiberglass was most likely physically originated. Amount of deposits increased during the tests. In test 3 where TSP was used, significant amount of phosphorous was found on the exterior surfaces of the submerged cal-sil samples. However in the interior parts of cal-sil, phosphorous was not detected with the same extent, which indicates that the phosphate diffusion in to cal-sil is limited. Sediment composed mainly of debris of insulation material, dirt, corrosion products and chemical precipitates. Amounts are presented earlier in *Table 3* and the high amounts of test 3 and 4 correlate with the cal-sil addition. Si was the dominant element in test 1, 2 and 5, where only fiberglass was present. In test 3 and 4 the presence of cal-sil resulted in a higher Ca percentage in the sediment than that of Si. TSP addition increased the amount of phosphorous in the sediment of test 2 and 3. (Chen et al., 2007)

The weight loss of unsubmerged metal and concrete coupons was insignificant. Biggest weight loss was detected in the submerged aluminium and uncoated steel coupons, and Al weight loss corresponded well with the concentration found in the solution. (Chen et al., 2007)

Two different kinds of precipitates were also detected. In test 3 during the TSP addition at 60 °C, white calcium phosphate precipitate was formed and in tests 1 and 5 aluminium borate precipitate was formed. These kinds of precipitates may be formed during the cool down and it is possible that they do not redissolve even when the temperature rises again. Also the temperature profile in pool, ECCS or heat exchanger is not homogenous, and therefore precipitates may be formed at the low temperature regions and then be transported to the sump screen. (Chen et al., 2007)

This kind of in situ testing offers more comprehensive and less conservative view to the chemical effects that take place in the post-LOCA environment. To fully investigate and evaluate the synergistic chemical effects, plant-specific pool conditions must be evaluated.

5. Chemical effects in BWRs

BWR coolant is mostly pure water and does not contain boric acid. Therefore, the coolant chemistry is much simpler than that in PWR. However, sodium pentaborate (SPB) is added to some BWRs, which can result in similar chemical effects that are observed in PWRs. Never the less in the post-LOCA conditions, high temperature and pH changes that result from the radiolysis of water may cause chemical reactions.

6. Testing of Chemical Effects

The post-LOCA sump water chemistry is very complex. A simple model or short-term testing alone cannot describe and evaluate all synergistic chemical effects that may occur in complex multicomponent environments. Laboratory tests are usually excessively conservative, since laboratory tests must be kept relatively simple to assess the influence of pH, temperature, concentration, ionic strength etc. Also exact simulation of some parameters, such as surface area to solution ratio, mass transport, rate of chemical addition, are not achievable in most tests. Since testing and further evaluating of chemical effects is so complex, the US NRC has developed an evaluation process (Figure 7) (US NRC, 2007).
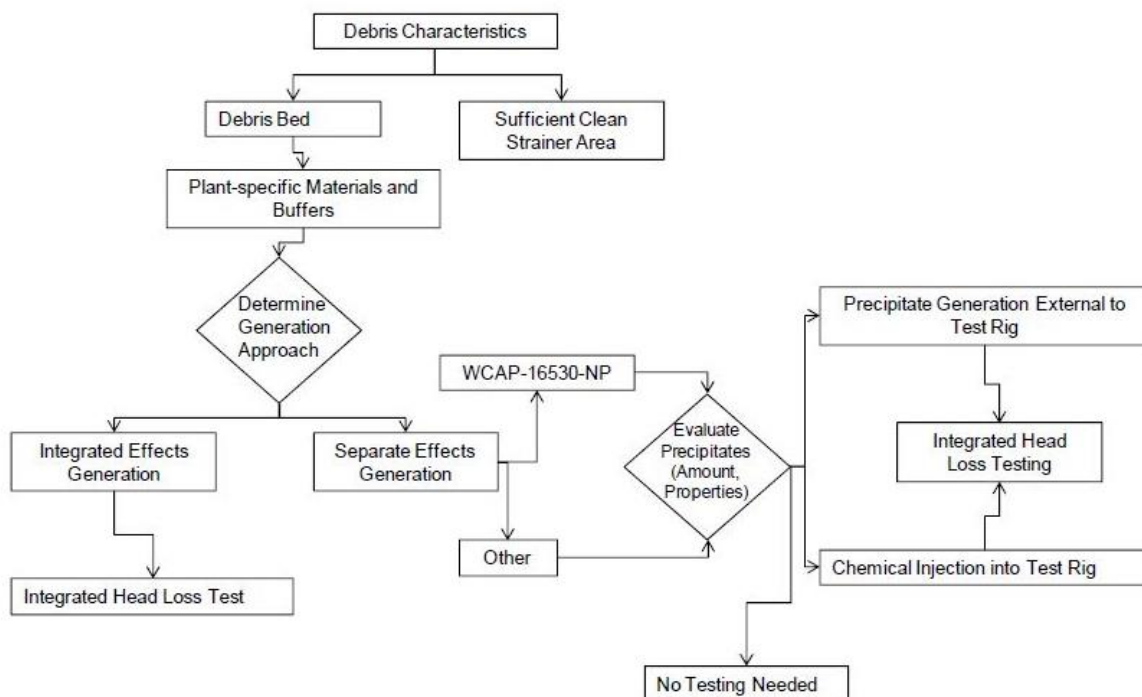

Figure 7. The evaluating process of Chemical Effects from US NRC (US NRC, 2007).

6.1 Analytical methods

The chemical tests have been experimentally evidenced by small scale bench test, integrated chemical effects tests (ICET) or *in situ* tests and also with vertical loop head loss tests (Bahn, 2013). Chemical effect testing often begins with analysing of plant specific conditions and with the production of precipitates or surrogates. Production and characterisation of these precipitates is usually conducted in bench experiments. Then larger scale *in situ* tests are conducted to simulate the reactor pool environment and to evaluate synergistic effects so that all passivation/inhibition/activation reactions will be included. Modelling is also often used to characterise the precipitates etc. Larger scale *in situ* experiments include solution analysis during and after the experiment and characterisation of the solids at least before and after the experiment. Precipitates may be further analysed with separate single effect testing with subsequent surface and solid state characterisation.

6.1.1 Test equipment

6.1.1.1 Single effect bench-scale tests

Single effect test for example precipitation tests may be conducted with relatively simple equipment. Reflux equipment with heating system has been described by *Bahn et al.* Heating system was designed to produce temperature program that simulates heat up and cool down of the coolant. Figure 8 show a picture of test equipment. (Bahn et al., 2011a)

Figure 8. Long term Al hydroxide precipitation tests (Bahn et al., 2011a).

Bench-scale test are usually used to analyse for example precitation of sertain precipitate in contrast of temperature evaluation or dissolution of sertain containment material. Also further characterisation with some solid state characterisation method is often used for the created precipitate. Single effects tests are usually conservative due to the fact that passivation or inhibition reactions cannot be evaluated.

6.1.1.2   *In situ* tests

Larger scale (e.g *in situ*) tests are usually more complex and intension is to simulate expected containment pool chemistry during the recirculation after LOCA including all possible interactions that might occur. Therefore, the test system is more complex and includes often a test tank made of stainless steel with heating elements and spray nozzles (diagram presented in Figure 9).
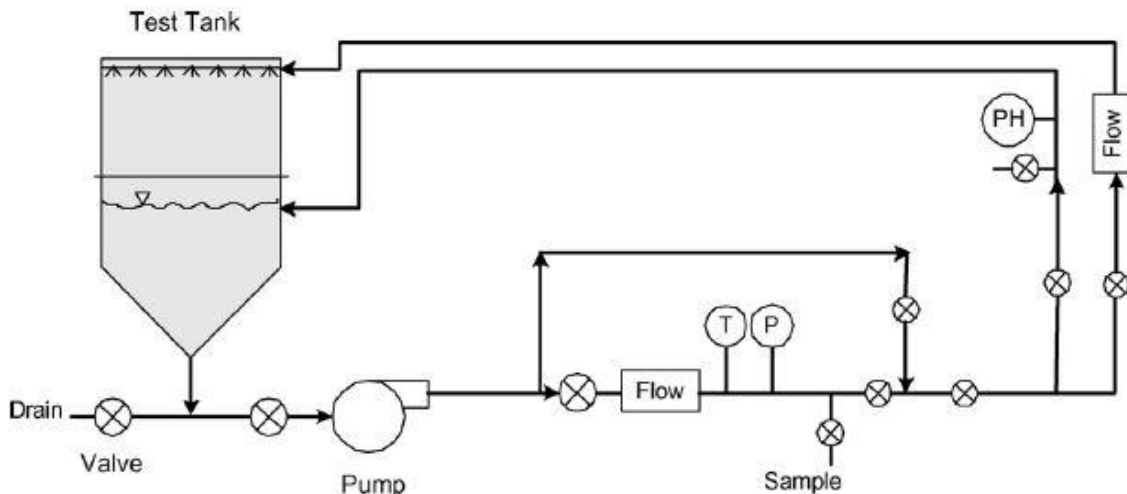

Figure 9. Diagram of the in situ test equipment (Dallman et al., 2006a)

In tank, there will be all materials that can be found in the sump water pool, e.g. aluminium alloy, carbon steel, galvanised steel, zinc coated steel, copper, concrete as a pulver and slab, pipe insulation materials, dust and other latent debris materials. Solution chemicals are boron as H_3BO or sodium tetraborate, LiOH or other alkali hydroxide, HCl and pH buffer (TSP, NaOH or SMB) and the deionised water as base solution. Materials and chemicals are scaled in proportion to actual contitions in operating nuclear power plant. Test equipment often icludes on line monitoring of flow rate, pH and temperature (Figure 9). Also system for collecting solution and dissolved species samples is often required (Figure 9).

Figure 10. Metal, concrete etc. loaded on racks in ICET test tank. (Dallman et al., 2006a)

Metal and concrete coupons have been placed in chlorinated polyvinyl chloride racks to ensure sufficient space between the coupons and prevent the galvanic interactions among the coupons (Figure 10). Then representative amounts of racks are either submerged into the test solution or were placed above the water level (unsubmerged). Other solid materials, such as latent debris, concrete, insulation material samples are placed in the tank. The metal coupons and other solid species (insulation material, sediment and precipitates) are often characterised with different kinds of surface characterisation methods before and after the experiment. (Chen et al., 2007; Dallman et al., 2006a; Zhang et al., 2009). Some of these methods are presented later.

6.1.1.3   Loop type head loss tests

The formation and evaluation of precipitates if often tested by strainer or debris bed head loss testing. Important features of the precipitates, such as filterability, characteristics, particle size, settlement rate etc. can be investigated by loop type head loss testing (Figure 11). (Bahn et al., 2009) In head loss tests, the horizontal configuration of the strainer does not reflect the realistic strainer configuration, but rather to permit the formation of uniform debris beds with well-defined characteristics (Bahn, 2013).

In loop experiments, precipitates or surrogates are prepared in advance and added to the experiment loop after debris bed and solution are placed in the loop. Since, the precipitates are prepared in advance it is possible that they do not fully correspond to the precipitates that are formed during actual post-LOCA environment. For example the solution concentration affects the particle size of the precipitation. However, particle size and other characteristics of produced precipitates are often well analysed before the loop experiments. (Bahn et al., 2009) Corrosion tests of Al alloys with head loss testing have also been conducted with similar test setups (Bahn et al., 2011b). Results have shown that particle size of formed Al precipitate has significant effect on the strainer head loss. If only nm scale precipitation is formed, effect on head loss can be minimal (Bahn et al. 2011a; Bahn et al., 2011b).
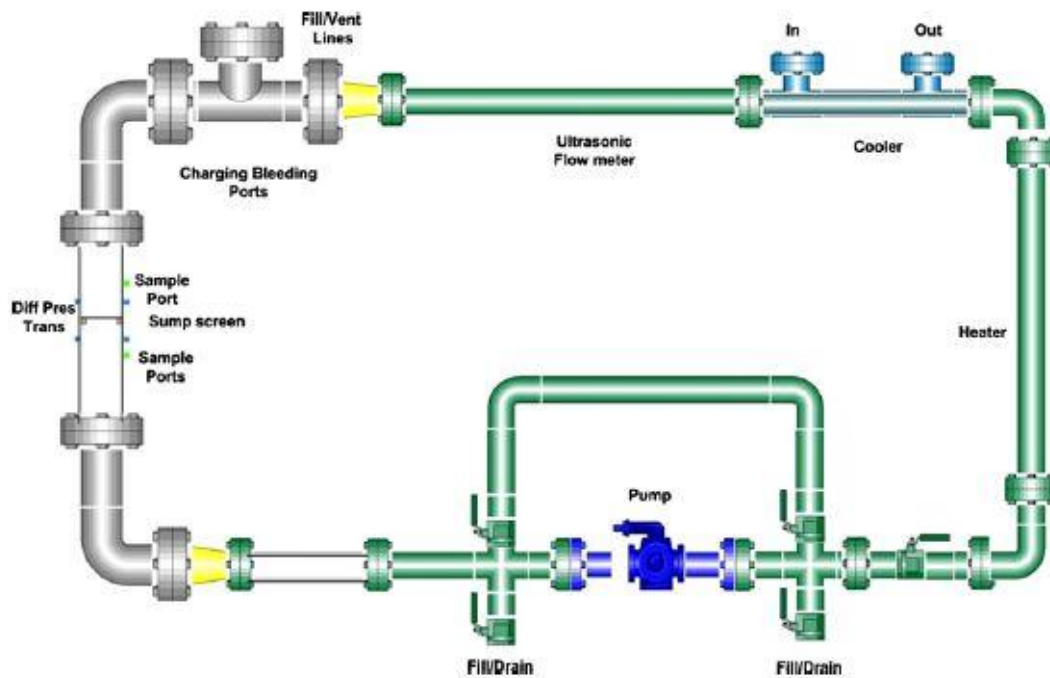
Figure 11. An example of schematic picture of head loss testing loop. (Bahn et al., 2009)

Experimental test loop or other equipment is usually cleaned entirely so that all old deposits and residues will be removed and will not remain from the previous tests. The cleaning procedure often requires flushing with alkaline and acid solution, also with organic solvent and deionized water to remove all impurities. *Chen et al.* reported loop cleaning procedure by flushing with ammonium hydroxide, ethanol, dilute nitric acid and demineralised water (Chen et al., 2007).

Loop tests have shown that the head loss depends on the amount and size of the particulate material. The greater the particulate amount collected on strainer is, the greater is the resulting head loss. Head loss is also roughly linearly dependent on the particulate volume. For the fibrous debris, larger quantities seem to lower the head loss, and only at very large quantities the head loss increases with the increasing fibre quantity. The screen or strainer surface area is powerful control in sump screen design. Therefore, increasing the surface area of the screen can effectively reduce the head loss across the sump screen during post-LOCA conditions. (Hart et al., 2004)

Also when particles deposit on the fibre debris rather than mix completely with debris before deposition, the head loss is larger and sharp increase in head loss was detected after sufficient amount of colloids was deposited on the debris. However, head loss may be suppressed by the hydrochloric acid corrosion of rock wool and enlarging of the sump screen (NEA, 2013); (Park et al., 2009).

6.1.2   Solution analytics

Solution analyses are often made by continuous on line monitoring. pH, temperature, and flow velocity in the case of loop testing is necessary to conduct with on line monitoring. Also *Chen et al.* reported solution features such as turbidity, total suspended solids, kinematic viscosity and elemental composition that were analysed with inductively coupled plasma atomic emission spectrometry (ICP-AES) by daily bases from the ICET test solution. The analysed elements were Al, Ca, Si, B, Na, Fe, Zn, Mg and Cu. (Chen et al., 2007; Dallman et al., 2006a)

6.1.3   Characterisation of surfaces, precipitates and sediments

Solid metal and concrete coupons, precipitates, fiberglass and cal-sil debris and sediments are often analysed with scanning electron microscope and energy dispersive spectroscopy (SEM/EDS). Also X-ray methods; X-ray photoelectron spectrometry (XPS), X-ray diffraction (XRD) and X-ray fluorescence (XRF) are used for the characterisation of the precipitates and sediments. Other methods such as atomic force microscopy (AFM) and particle size distribution methods have also been used, but they are not presented in this literary review.

6.1.3.1   SEM

SEM technique is often used for analysing solid samples and surface structures. *Chen et al.* used SEM to analyse the corrosion of aluminium by analysing the surfaces of aluminium alloy coupons before and after soaking in the test solution. Tests were conducted in the *in situ* manner to evaluate synergistic effects in the post-LOCA environment. Test were conducted with few variable parameter, such as NaOH, TSP and sodium tetraborate addition, buffer amounts were varied and therefore also pH varied, and also the amounts and types of insulation materials were changed to simulate different plant systems. Test solution conditions with details are presented in the *Table 4 and* SEM images of Al alloys are presented in *Figure 12*. Solution temperature was kept at about 60 °C, circulation velocity was 94.6 L/min and tests were run for 30 days.

Table 4. Results of aluminium corrosion tests by Chen et al. (data from Chen et al., 2008)

| Added [mg/L]	Test 1	Test 2	Test 2	Test 3	Test 5
H_3BO_3	16,000	16,000	16,000	16,000	16,000
NaOH	7677	-	-	9600	-
$Na_3PO_4 \cdot 12H_2O$	-	4000	4000	-	-
$Na_2B_4O_7 \cdot 10H_2O$	-	-	-	-	10,580
HCl	100	100	100	100	43
LiOH	0.7	0.7	0.7	0.7	0.3
Fiberglass	5270	5270	1050	1050	5270
Cal-sil	-	-	20,800	20,800	-
Pulverised concrete/debris	90	90	90	90	90
Results					
pH	9.3 – 9.5	7.1 – 7.4	7.3 – 8.1	9.5 – 9.9	8.2 – 8.5
Al in solution	360	< LOD	< LOD	< LOD	50
Mass loss from coupons [g]	296	2.7	< 0.1	< 0.1	33.6
Corrosion rate ($g \cdot m^{-2} \cdot h^{-1}$)	1.40 (in 18 days)	0.007	< 0.001	< 0.001	0.25 (in 14 days)
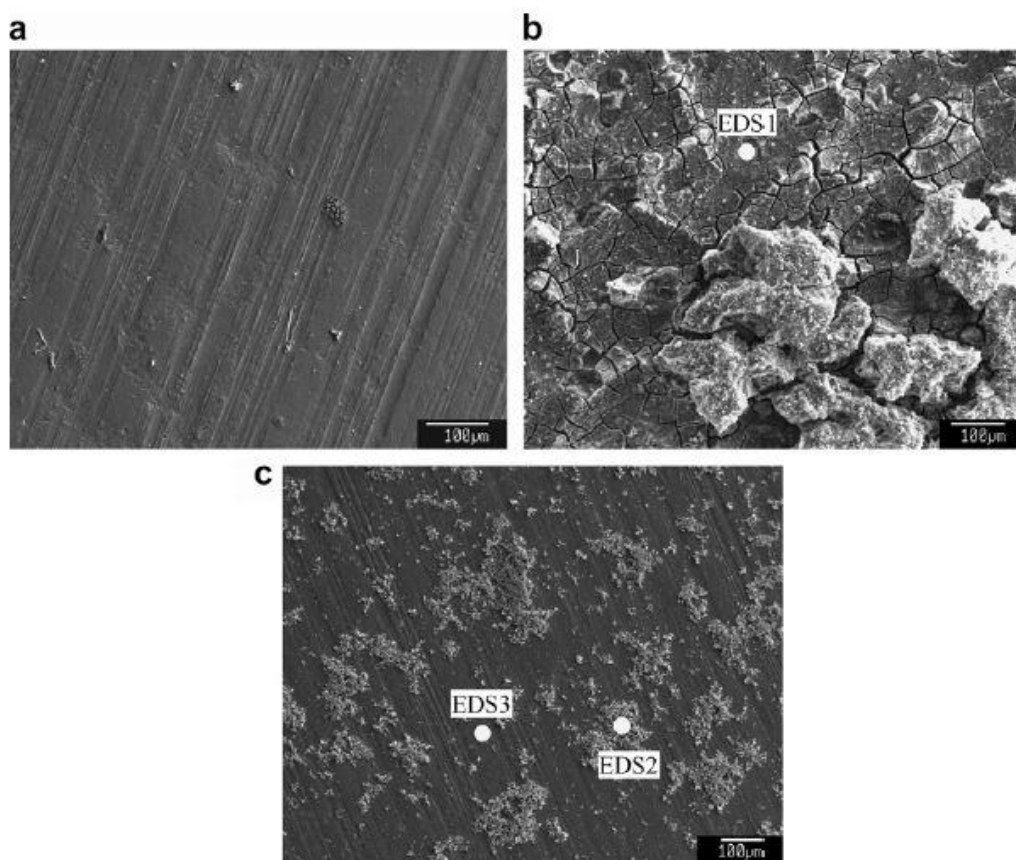
Figure 12. SEM images of Al alloy coupons a) new coupon, before testing, b) Al coupon surface with a lot of corrosion products and c) Al coupon with only little corrosion, after testing (Chen et al., 2008).

The fresh Al alloy SEM picture (Figure 12a) shows clean surface without corrosion products. *Figures 12b* and *c* show the surface of Al coupon after 30 days of submersion in the test solution (b corresponds to Test 1 and c to test 4). In test 1, the solution contained borate, NaOH, HCl, LiOH, fiberglass insulation material and pulverised debris. Measured pH was 9.3 – 9.5 and measured corrosion rate of Al was 1.40 $g \cdot m^{-2} \cdot h^{-1}$, which was the highest measured corrosion rate in the tests of *Chen et al.* SEM picture of the Al coupon from test 1, show extensive amount of corrosion products, which corresponds well with the measured high corrosion rate. The SEM picture of test 4 Al coupon shows just a small amount of corrosion product on the coupon surface. Test 4 solution was primarily similar with the test 1 solution, but test 4 contained mostly cal-sil insulation material instead of fiberglass. Measured pH was 9.5 – 9.9 and corrosion rate of Al was very low; less than 0.001 $g \cdot m^{-2} \cdot h^{-1}$. Low amount of corrosion products correlated well with the low corrosion rate. (Chen et al., 2008)

To evaluate surfaces more and find out whether Si or Ca passivation happened on the surface of the test 4 coupon, semi-quantitative chemical composition analyses were made with EDS (Chen et al., 2008). *Figures 12b* and *c* show the EDS points and results of EDS analyses are presented in *Table 5*.

Table 5. EDS analyses results of soaked Al coupons [w/w%] (compare with Figure 12b and c) (modified from Chen et al., 2008)

Element	Al	O	Si	Ca	Na	B	Mn	C	Mg
EDS1	18	61	2	5	2	9	3	-	-
EDS2	10	58	9	10	10	-	-	2	2
EDS3	75	21	4	1	-	-	-	-	-

All EDS points of the test 1 and 4 coupons contained mainly Al and O, which indicates Al oxide or hydroxide surface. EDS3 point elemental composition corresponds primarily with fresh Al alloy surface without corrosion products. In EDS2 point, in addition to Al and O, Si, Ca and Na were detected, but the amounts of Ca and Si were not so significant and EDS1 from the test 1 contained also small amounts of Si and Ca, so conclusions about the passivation effects could not be made with only based on the SEM and EDS analyses. (Chen et al., 2008)

6.1.3.2   XPS

XPS can be used to analyse surface characteristics and elemental speciation on the solid surface. *Klasky et al.* used XPS to analyse the possible Si passivation reaction. XPS spectra for new aluminium alloy coupon and for Al coupon soaked for 30 days in Na_2Sio solution are presented in *Figure 13*. (Chen et al., 2008; Klasky et al., 2006)
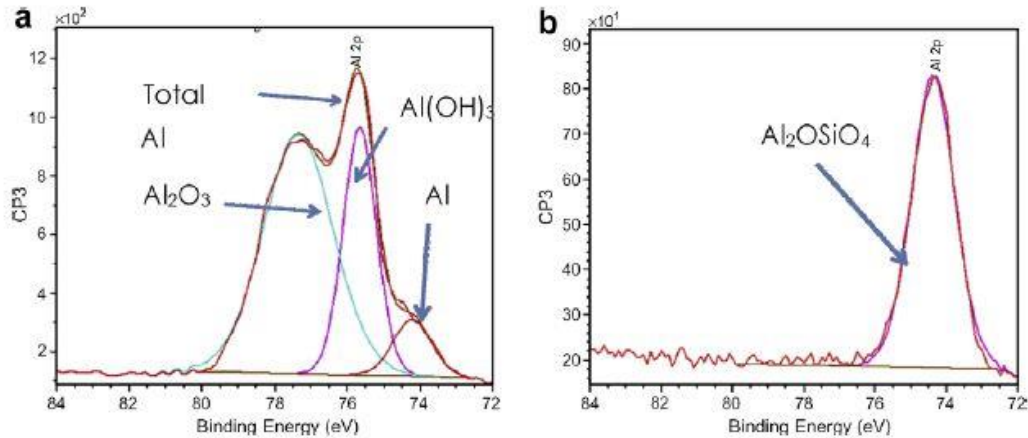

Figure 13. XPS spectra to the depth of 10 nm of Al alloy a) new coupon and b) soaked in Na_2SiO solution (Chen et al., 2008; Klasky et al., 2006)

XPS spectrum (Figure 13a) of fresh Al alloy coupon shows characteristic Al surface structures. Small part (9 %) of the surface is metallic aluminium, the biggest part (64 %) is protective oxide surface layer (Al_2O_3) and a part (27 %) of the oxide layer has transformed to aluminium hydroxide. This effect has been explained also previously in this report in the aluminium corrosion section. In the spectrum of soaked Al coupon (Figure 13b), the surface of the coupon consists mainly on Al_2OSiO_4 (98 %) and only 2 % is present as Al_2O_3. This indicates that in silicate solution, silicate passivation layer is formed which covers completely the metallic Al and therefore prevents the Al corrosion. Further tests have shown that the Si passivation layer is stable under alkaline conditions (pH 9.5). (Zhang et al., 2009)

6.1.3.3 XRD

XRD can be used to analyse atomic and molecular structure on the solid surface. With XRD technique three-dimensional picture of electron density within the crystal can be formed and further the locations of atoms and form of chemical bonds may be analysed. *Zhang et al.* presented an example of aluminium hydroxide analysis with XRD and spectrum is presented in *Figure 14.* Al hydroxide was produced by titrating ammonium into Al chloride solution to pH 7. (Zhang et al., 2009)
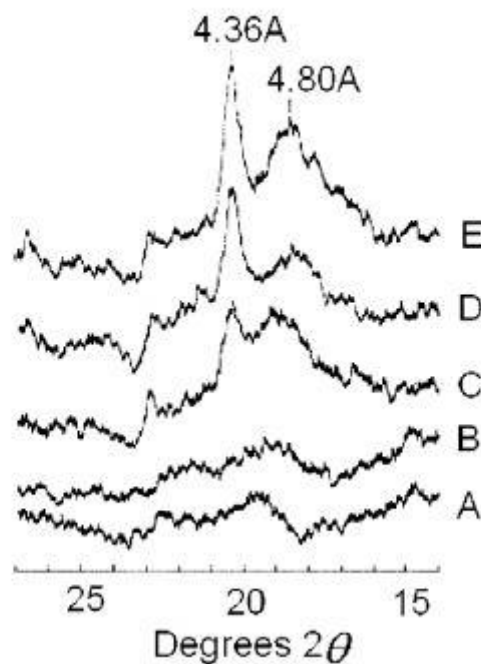

Figure 14. XRD pattern of Al hydroxide gel during aging at pH 7 and 25 °C. With time A) 56 d, B) 78 d, C) 94 d, D) 115 d and E)189 d. (Zhang et al., 2009)

Figure 14 shows that XRD pattern changes significantly due to the aging effect. (Zhang et al., 2009) Amorphous solids result in continuous XRD spectrum and characteristic peaks do not show in the spectra. In result of aging, the crystallinity of Al hydroxide increases and two characteristic peaks began to appear in the XRD spectrum. Longer aging time results in more crystalline precipitate and more characteristic XRD spectrum with peaks that can be identified.

7. Summary and conclusions

Emergency cooling water sump contains many elements that may form precipitates. However, dissolution test have shown that elements such as Mg and Ti have so low solubility and that it is unlikely that they form precipitates. Zn and Fe corrode and are released into the sump. However, the amounts of these are relatively low, so that the amount of Zn or Fe precipitates would probably also be low compared with the precipitates of Al, Si, Ca and PO_3 (see Figure 15). *Figure 15* shows the comparison of the amounts of different elements that undergo dissolution in containment pool environment (Lane et al., 2008).
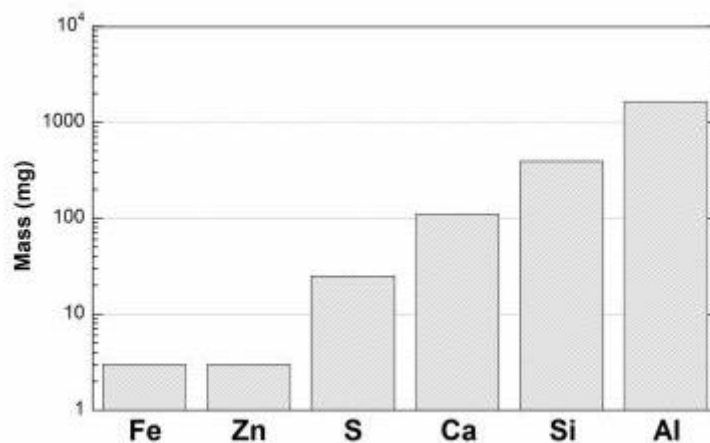

Figure 15. Total masses of released elements due to the dissolution (Lane et al., 2008). Results from dissolution tests are not exact masses in containment pool, but diagram gives the relative amounts of elements so that they can be compared to each other.

Aluminium, silicate and calcium have the highest concentration in the solution. Therefore, their precipitates are the most problematic under post-LOCA sump conditions considering the strainer blockage and head loss. Three main chemical precipitates that are most probable to form during post-LOCA environment are calcium phosphate, aluminium oxyhydroxide and sodium aluminium silicate. Also aluminium borates may be formed, when boric acid is used as solution additive in sump water. However, the formation of these is highly dependent on the conditions, for example phosphates are not precipitating without the use of phosphate buffer such as TSP. (Lane et al., 2008)

Comprehensive ICETs have shown that Al alloy is the most susceptible under simulated LOCA conditions, especially with high pH (Bahn et al., 2011; Chen et al., 2008). Also high water flow velocity increases the metal corrosion (Zhang et al., 2009) Boric acid in sump water increases significantly Al corrosion rate and solubility of Al hydroxides and oxyhydroxides. However, if sodium tetraborate is used as pH control and reactivity control agent, the effect of borate is significantly lower. However, the Al corrosion may be inhibited by silicate or phosphate and therefore the assumption that all released Al will form precipitate is highly conservative. Also various publications suggest that significant amount of dissolved Al would stay in solution as extremely small colloids, which would not increase the head loss across the debris bed and strainers (Bahn, 2013; Bahn et al., 2008; Chen et al., 2008; Dallman et al., 2006a; Lane et al., 2008; Reid et al., 2007). On the contrary, all released calcium would probably form precipitate so therefore cal-sil insulation material amount should be minimised when TSP is used as a pH buffer.

In head loss tests, it has been reported that the major factors that could lead to significant increase of head loss, such as NaOH-buffered solutions caused greater head loss increase than N_2H_4-bufferes solutions and carbon steel corrosion can increase head loss significantly. Therefore, instead of NaOH and TSP buffers such as sodium tetraborate (SMB) and STB have been recommended. (Bahn, 2013) STB have also reported to allow higher solubility of Al (Reid et al., 2007).

In each plant, plant-specific containment materials, concentrations of soluble species and debris, pH, temperature during and after the accident determine the type and amount of chemical precipitates, which may form in the containment sump water. In order to investigate the chemical effects, containment materials, their dissolution rates, buffer compounds and plant-specific pH and temperature conditions must be investigated. (Lane et al., 2008) Local or general cooling is often a factor that triggers the formation of precipitation. Although it is possible that precipitates form also at higher temperatures. Precipitation at lower temperature may be irreversible so that precipitates will not redissolve if temperature rises again. Aging effects of the formed precipitates may be important if the cooling takes place over a long period of time. However, if the reaction kinetics are slow aging will not occur during the time frame of LOCA. But during long periods of emergency cooling, which took place for example in Fukushima the aging effect may become realistic.

pH in the pool is a very significant parameter and it has strong influence on the mass and volume of the formed precipitate. pH also significantly effects on the corrosion and dissolution of the containment materials. At pH 8.4 – 8.8 the amount of precipitates is significantly lower than that in higher pH, such as 9.3. Temperature higher in the range 50 – 55 °C has been reported to promote the formation of precipitates. Also containments materials, such as paint seems to have relatively low corrosion and therefore also low effect on the precipitate formation. (Sandrine et al., 2008)

Bahn reviewed the additional chemical phenomena that NRC-sponsored panel reviewed in order to identify the issues and phenomena that remain still unresolved. Most important features were the effect of organic materials (coatings and lubricants) with inorganic materials, the effect of radiolysis on the redox potential of metals and further their corrosion and also the effect of biological growth and dried borate salts on hot fuel cladding and reactor pressure vessel materials. Also the effects on the fuel and fuel cladding, and further to core cooling have been evaluated to be issues that need to be investigated more. (Bahn , 2013)

In the case of Finnish PWR, in addition to all previously described phenomena also the use of KOH in the sump water should also be considered. Reference for such studies with KOH as an additive in sump water cannot be found due to the fact that it is not used as an additive in PWR's very often, at least not in countries where information could be found easily. (NEA, 2013)

References

Bahn, C.B. 2013. Chemical effects on PWR sump strainer blockage after a loss-of-coolant accident: Review on US research efforts. Nuclear Engineering and Technology, Vol. 45, No. 3, pp. 295-310.

Bahn, C.B., Kasza, K.E., Shack, W.J., Natesan, K. & Klein, P. 2011a. Evaluation of precipitates used in strainer head loss testing: Part III. Long-term aluminium hydroxide precipitation tests in borated water. Nuclear Engineering and Design, Vol. 241, No. 5, pp. 1914-1925.

Bahn, C.B., Kasza, K.E., Shack, W.J., Natesan, K. & Klein, P. 2011b. Evaluation of precipitates used in strainer head loss testing: Part II. Precipitates by in situ aluminium alloy corrosion. Nuclear Engineering and Design, Vol. 241, No. 5, pp. 1926-1936.

Bahn, C.B., Kasza, K.E., Shack, W.J., Natesan, K. & Klein, P. 2009. Evaluation of precipitates used in strainer head loss testing. Part I. Chemically generated precipitates. Nuclear Engineering and Design, Vol. 239, No. 12, pp. 2981-2991.

Bahn, C.B., Kasza, K.E., Shack, W.J.& Natesan, K. 2008, Aluminium Solubility in Boron Containing Solutions as a Function of pH and Temperature. Argonne National Laboratory Report.

Chen, D., Howe, K.J., Dallman, J. & Letellier, B.C. 2008. Corrosion of aluminium in the aqueous chemical environment of a loss-of-coolant accident at a nuclear power plant. Corrosion Science, Vol. 50, No. 4, pp. 1046-1057.

Chen, D., Howe, K.J., Dallman, J., Letellier, B.C., Klasky, M., Leavitt, J. & Jain, B. 2007. Experimental analysis of the aqueous chemical environment following a loss-of-coolant accident. Nuclear Engineering and Design, Vol. 237, No. 20, pp. 2126-2136.

Choromokos, R., Mast, P. & Park, J.M. 2010. " Chemical Effect" Head Loss Pressure Drop for the Nuclear Power Plant Safety. ECS Transactions, Vol. 28, No. 24, pp. 37-59.

Chung, Y.W.; Cho, J.S.; Kwon, B.I.; Ku, H.K.; Choi, Y.J.; Kim, H.T. 2011, Development of Methodology for Evaluation of Chemical Effects on Sump Screen Performance Testing, Korea Nuclear Society Spring Meeting, May 26~27, 2011.

Dallman, J., Letellier, B., Garcia, J., Madrid, J., Roesch, W., Chen, D., Howe, K., Archuleta, L., Sciacca, F., December 2006a. Integrated chemical effects test project: consolidated data report, vol. 1. The U.S. Nuclear Regulatory Commission, NUREG/CR-6914.

Dallman, J., Garcia, J., Klasky, M., Letellier, B., Howe, K., December 2006b. Integrated chemical effects test project: Test 1 data report, vol. 2. The U.S. Nuclear Regulatory Commission, NUREG/CR-6914.

Dallman, J., Letellier, B., Garcia, J., Klasky, M., Roesch, W., Madrid, J., Howe,K., Chen, D., December 2006c. Integrated chemical effects tests: Test 2 data report, vol. 3. The U.S. Nuclear Regulatory Commission, NUREG/CR-6914.

Dallman, J., Letellier, B., Garcia, J., Madrid, J., Roesch, W., Chen, D., Howe,K., Archuleta, L., Sciacca, F., December 2006d. Integrated chemical effects tests: Test 3 data report, vol. 4. The U.S. Nuclear Regulatory Commission, NUREG/CR-6914.

Dallman, J., Letellier, B., Garcia, J., Madrid, J., Roesch, W., Chen, D., Howe,K., Archuleta, L., Sciacca, F., December 2006e. Integrated chemical effects tests: Test 4 data report, vol. 5. The U.S. Nuclear Regulatory Commission, NUREG/CR-6914.

Dallman, J., Letellier, B., Garcia, J., Madrid, J., Roesch, W., Chen, D., Howe,K., Archuleta, L., Sciacca, F., December 2006f. Integrated chemical effects tests: Test 5 data report, vol. 6. The U.S. Nuclear Regulatory Commission, NUREG/CR-6914.

Griess, J. & Bacarella, A. 1969. Design Considerations of Reactor Containment Spray Systems - Part III. The Corrosion of Materials in Spray Solutions. Oak Ridge National Laboratory, Oak Ridge, Tennessee.

Hart, G.H. 2004. A short history of the sump clogging issue and analysis of the problem. Nuclear News, Vol. 47, No. 3, pp. 24-34.

Jain, V., He, X. & Pan, Y.M., 2005. Corrosion Rate Measurements and Chemical Speciation of Corrosion Products Using Thermodynamic Modelling of Debris Components to Support GSI-191, NUREG/CR-6873, The US Nuclear Regulatory Commission, Washington DC.

Klasky, M., Zhang, J., Ding, M., Letellier, B., Chen, D. & Howe, K. 2006. Aluminium chemistry in a Prototypical Post-Loss-of-Coolant-Accident, Pressurized-Water-Reactor Containment Environment, NUREG/CR-6915, The US Nuclear Regulatory Commission, Washington DC.

Lane, A.E., Andreychek, T.S., Byers, W.A., Jacko, R.J., Lahoda, E.J. & Reid, R.D. 2008. Evaluation of Post-Accident Chemical Effects in Containment Sump Fluids to Support GSI-191. Westinghouse Report WCAP-16530-NP-A.

NEA 2013, Updated Knowledge Base for Long Term Core Cooling Reliability, NEA/CSNI/R(2013)12, pp. 127-172

Park, J.W., Park, B.G. & Kim, C.H. 2009. Experimental investigation of material chemical effects on emergency core cooling pump suction filter performance after loss of coolant accident. Nuclear Engineering and Design, Vol. 239, No. 12, pp. 3161-3170.

Piippo J., Laitinen T. & Sirkiä P. 1997 Corrosion behaviour of zinc and aluminium in simulated nuclear accident environments. STUK-YTO-TR 123. Helsinki: Radiation and Nuclear Safety Authority.

Reid, R.D., Crytzer, K.R. and Lane, A.E., 2007. Evaluation of Additional Inputs to the WCAP 6530-NP Chemical Model, Westinghouse Report WCAP-16785-NP-A.

Sandrine, R., Cantrel, L., Yves, A., Jean-Marie, M., Marek, L., Dagmar, G., Yvan, V. & Bela, S. 2008. Precipitate formation contributing to sump screens clogging of a nuclear power plant during an accident. Chemical Engineering Research and Design, Vol. 86, No. 6, pp. 633-639.

US NRC, 2007. Evaluation Guidance for the Review of GSI-191 - Plant-Specific Chemical Effect Evaluations, U.S. Nuclear Regulatory Commission, 2007.

Zhang, J., Klasky, M. & Letellier, B.C. 2009. The aluminum chemistry and corrosion in alkaline solutions. Journal of Nuclear Materials, Vol. 384, No. 2, pp. 175-189.